Available online at www.sciencedirect.com
ScienceDirect
Journal of the European Ceramic Society 30 (2010) 737–742
www.elsevier.com/locate/jeurceramsoc

Evolution of the intergranular phase during sintering of $CaCu_3Ti_4O_{12}$ ceramics

J.J. Romero [a,*], P. Leret [a], F. Rubio-Marcos [a], A. Quesada [b], J.F. Fernández [a]

[a] *Instituto de Cerámica y Vidrio, CSIC, C/Kelsen 5, 28049-Madrid, Spain*
[b] *Dpto. Física de Materiales e Instituto de Magnetismo Aplicado, Universidad Complutense de Madrid, 28240-Madrid, Spain*

Received 5 February 2009; received in revised form 20 August 2009; accepted 27 August 2009
Available online 25 September 2009

Abstract

$CaCu_3Ti_4O_{12}$ (CCTO) ceramics have been processed by solid state reaction and sintered at 1100 °C for different times. A clear increase of the dielectric constant of the material up to values of 6×10^4 has been observed with the sintering time. This increase is accompanied by a limited grain growth and intergranular Cu-oxide phase thickness reduction. The disappearance of the Cu-oxide phase is caused by the incorporation of Cu cations into the grains, contributing to the increase of the dielectric constant. Raman spectroscopy shows the decrease of TiO_6 octahedral rotational modes with the sintering time due to the incorporation of Cu cations into the CCTO grains. XANES measurements show that the Cu main oxidation state is Cu^{2+} and does not change with the sintering time. The fitting of the experimental dielectric constant to the Internal Barrier Layer Capacitance (IBLC) model reveals the change of the intergranular phase dielectric constant, caused by a compositional change due to the incorporation of Cu into the CCTO grains.

Keywords: Dielectric properties; Perovskites; Sintering

1. Introduction

The recent observation by Subramanian et al.[1] of a giant dielectric constant in calcium copper titanate, $CaCu_3Ti_4O_{12}$ (CCTO), has led to considerable efforts aimed to understand the origin of this behaviour. The high frequency dielectric constant of about 10^4–10^5 is practically frequency independent between DC and 10^6 Hz and possesses good temperature stability over a range from 100 to 400 K.[1–4]

CCTO shows an Im3 space group,[1,5] derived from the ideal cubic perovskite structure by superimposing a body centered ordering of Ca and Cu ions and a pronounced tilting of the titanium centered octahedra. This tilting alters the coordination of Ca and Cu cations, leading to a square-planar environment for Cu and 12-coordinate icosahedral for Ca. The Cu–O distances show no variation with temperature (in the range 50–300 K), due to the high rigidity of these bonds.[6]

Although the large number of works published about this material, there is still no commonly accepted model explaining the obtained values of dielectric constant (ε) shown by CCTO, mainly due to the discrepancy of the obtained results even for materials prepared in a similar way. Some authors propose intrinsic defects, such as stoichiometry variations,[7] oxygen vacancies, presence of twinnings[8] or aliovalences of Ti and Cu ions,[9] as the source of the observed values of ε. These defects should be inherent to the material, though the preparation process can affect their quantity or even nature. On the other hand, some other authors propose the presence of secondary phases that form layered structures giving rise to an enhancement of the material's dielectric constant, as stated out by the Internal Barrier Layer Capacitance (IBLC) model.[10] This model is commonly accepted for ceramic samples[4] and also on thin films.[11] In the case of single crystals the presence of such layered structures is highly controversial, although it has been recently proposed that defect structures form layers that give rise to an IBLC-like effect.[12]

The nature of the proposed barriers has still not been fully characterised. Most authors associate them in ceramic samples to the intergranular material,[13] although some other structures, as intrinsic twin boundaries, have also been proposed.[8] The inter-

* Corresponding author.
E-mail address: jjromero@icv.csic.es (J.J. Romero).

0955-2219/$ – see front matter © 2009 Elsevier Ltd. All rights reserved.
doi:10.1016/j.jeurceramsoc.2009.08.024

granular layers are composed mainly of Cu oxides, with small amounts of Ti and Ca oxides.[14] This Cu-oxide rich phase forms a liquid at the sintering temperature, being an important factor for the growth of the CCTO grains, which is mediated by the presence of the liquid phase. It has been demonstrated that the intergranular phase shows a higher resistivity than the grains interior.[15]

In this work, we analyze the effect of sintering time on the increase of the dielectric constant of CCTO and the intergranular phase composition. The increase of the dielectric constant is accompanied by grain growth and a decrease of the intergranular layer thickness. Moreover, a Cu concentration increase on the CCTO grains interior was observed with the sintering time.

2. Experimental procedure

$CaCu_3Ti_4O_{12}$ ceramics were prepared using a solid state reaction process followed by sintering at 1100 °C during different times. The analytical grade $CaCO_3$ (Aldrich), TiO_2 (Merck) and CuO (Aldrich) were mixed at the stoichiometric relation by attrition milling with 1.2 mm Zirconia balls for 2 h, using deionized water as liquid medium and 0.2% wt of Dolapix C64 as dispersant. The milled powders were dried and sieved through a 100 μm mesh and two times calcined at 900 °C for 4 h and attrition milled for 3 h. Organic binders (0.6% wt of polyvinyl alcohol, PVA, and 0.3% wt of polyethylene glycol, PEG) were added into the calcined powders upon final milling to help the formation of compacts. Powders were dried and sieved through a 63 μm mesh and uniaxially pressed at 200 MPa into discs of 8 mm in diameter and 1.3 mm in thickness. The pellets were sintered in air at 1100 °C for 2, 8, and 32 hours. Polished discs were electroded with fired silver paste to form a parallel plate capacitor.

The X-ray diffraction analysis was performed on a Siemens Kristalloflex diffractometer using $CuK\alpha_1$ radiation and Ni filter. The room temperature Raman scattering was excited using 514 nm radiation from an Ar^+ laser and collected by a microscopic Raman spectrometer (Jobin Yvon 64000). The microstructure of polished and thermally etched samples was observed using optical microscopy and a Hitachi S-4700 Field Emission Scanning Electron Microscope, FE-SEM. Image analysis was used to evaluate grain size distribution over more than 500 grains. The dielectric properties were measured at room temperature in the frequency range of 100 Hz to 1 MHz, using an Agilent 4294A impedance analyzer. Room temperature XANES spectra were performed at the SPLINE line of ESRF at the CuKα absorption edge on fluorescence configuration.

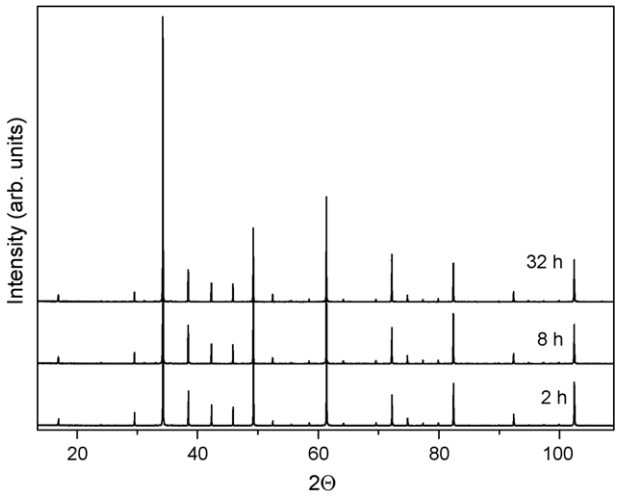

Fig. 1. X-ray diffraction of the CCTO ceramic samples sintered for different times.

3. Results and discussion

The XRD patterns of all CCTO ceramic samples, shown in Fig. 1, reveal a well crystallized perovskite structure with Im3 symmetry[5]; no other phases were detected by this technique. A slight reduction of the lattice parameter of the samples takes place with the sintering time, decreasing from 7.39 Å for 2 h sintering time to 7.37 Å for 32 h.

The grain size has been measured from optical micrographs of thermally etched samples sintered at different times, see Fig. 2.

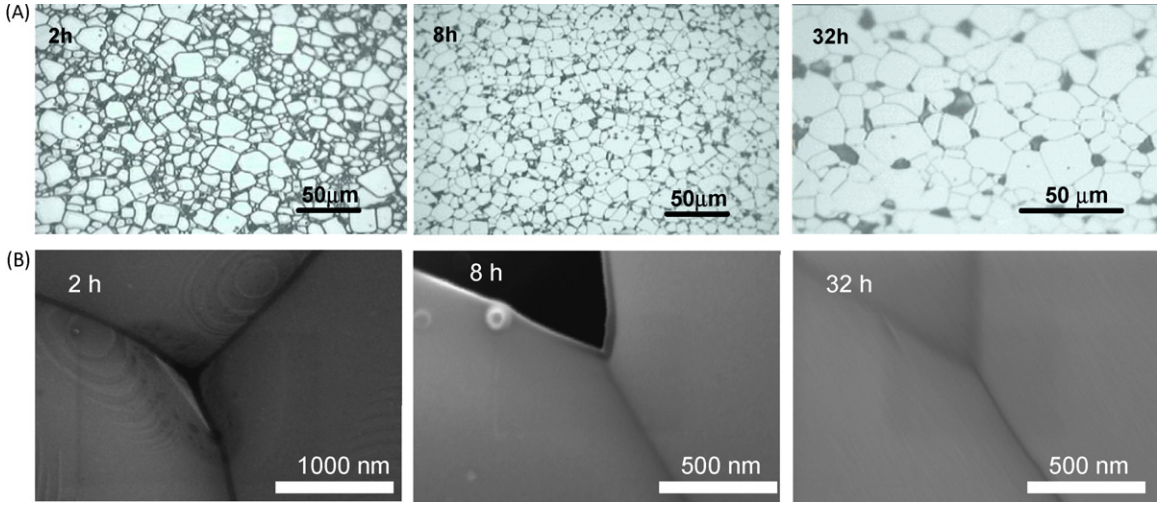

Fig. 2. (A) Optical micrographs of thermally etched samples sintered for 2, 8 and 32 h. (B) FE-SEM micrographs of the intergranular phase on the previous samples.

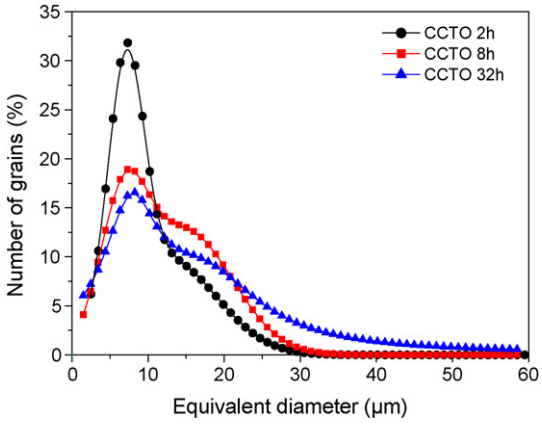

Fig. 3. Grain size distribution of the samples shown in Fig. 2.

The grains show a bi-modal size distribution, with small grains of nearly 8 μm equivalent diameter and larger grains of nearly 20 μm in all cases. The percentage of bigger grains increases with the sintering time (see Fig. 3).

The grain size increase is accompanied by the reduction of the dark, intergranular secondary phase, as can be observed on the FE-SEM micrographs shown in Fig. 2B. The thicknesses of these interphase regions have been measured, giving values of 45 ± 15 nm for 2 h sintered samples, and 29 ± 8 and 16 ± 5 nm for 8 and 32 h sintering times, respectively. These thicknesses have been obtained as an average of more than 20 different grain boundaries in all cases. The intergranular secondary phase is a CuO-rich phase, as shown by EDX measurements (CuO/TiO_2 approximately 96/4 on the sample sintered for 2 h, in good accordance with previous results[14]). The composition of the intergranular secondary phase on samples sintered for longer times could not be determined because of their small sizes. The obtained CuO/TiO_2 ratio corresponds to the eutectic composition that forms a liquid at 925 °C and assists the sintering during the early stages, causing exaggerated grain growth. The high homogeneity of the synthesized powders, attained by the double calcination step, reduced both the amount of secondary phase and the average grain size in respect to previous works.[14]

The composition of the crystalline grains on the different samples has been measured by EDX. In samples sintered for 2 h, the Cu/Ti ratio on the bigger grains is smaller than the stoichiometric one, being just 0.730 ± 0.007 (this result is the average of ten measures in different grains). At longer sintering times (32 h) this ratio increases up to 0.751 ± 0.009 (close to the stoichiometric ratio). These results indicate that Cu cations from the intergranular phase incorporate into the CCTO grains with the sintering time, making the CCTO grains to evolve approaching the stoichiometric composition. This fact implies that at short sintering time the crystal structure is off-stoichiometric and the charge neutrality of the perovskite must produce oxidation state changes and vacancies.

The room temperature Raman spectra of the samples sintered for different times has been measured, and the results corresponding to samples sintered for 2 and 32 h are shown in Fig. 4. Before discussing these results, we briefly summarize some properties of CCTO Raman spectrum. The material is a

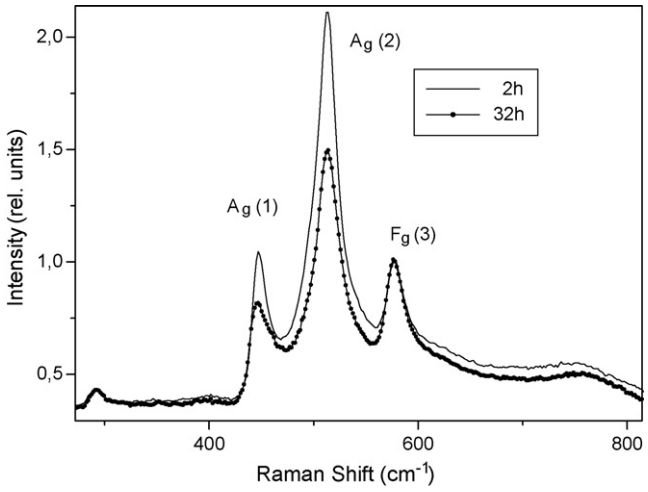

Fig. 4. Raman spectra of the samples sintered for 2 and 36 h. Both spectra are normalized to the antistretching vibration at 576 cm^{-1}.

weak scatterer and only five of the eight predicted symmetry modes are observed: the TiO_6 rotation-like modes, identified as A_g (1) (444 cm^{-1}), F_g (2) (453 cm^{-1}) and A_g (2) (510 cm^{-1}); the Ti–O–Ti antistretching mode of the octahedron, F_g (3) (576 cm^{-1}) and the F_g (4) (710 cm^{-1}) mode, assigned to the symmetric stretching breathing of the TiO_6 octahedron.[16]

The Raman spectra shown in Fig. 4 have been normalized to the intensity of the F_g (3) antistretching vibration of the O–Ti–O bonds. This peak has been used as reference since the Ti concentration on the samples is supposed to be nearly constant, while the Cu distribution changes as a function of the sintering time, due to observed increase on the Cu/Ti ion ratio in the grains. The Raman spectra obtained on all samples correspond to the previously described results for CCTO.[16] Upon increasing sintering time, the major difference observed in the spectra is the intensity reduction of the A_g (1) (444 cm^{-1}) and A_g (2) (510 cm^{-1}) bands, associated to rotation (or tilting) modes of the TiO_6 octahedron. These rotation movements of the TiO_6 octahedra would be highly influenced by the presence of Cu atoms on the lattice, since Cu–O bonds are very rigid[17] and should impede the

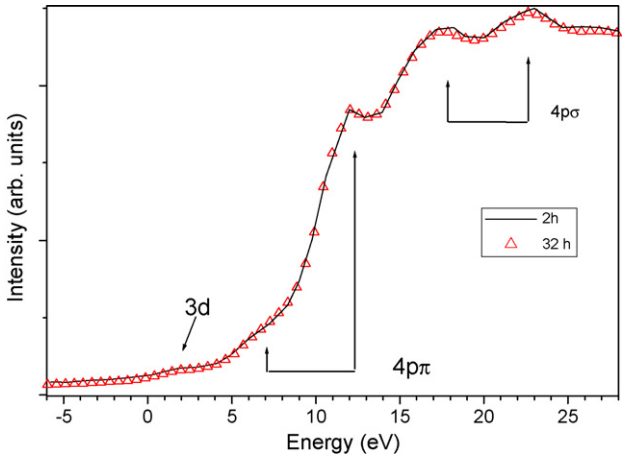

Fig. 5. XANES spectra of CCTO ceramic samples sintered for 2 (black line) and 32 h (open triangles). The final states of transitions departing from state 1s of Cu^{2+} ions are indicated.

rotation of the octahedrons. The reduction of the rotation modes intensity should then be associated to the observed incorporation of Cu into the crystal lattice with the sintering time.

In the long sintering time samples, the shape of these two rotational peaks is not symmetrical, showing the presence of new broad peaks appearing at longer Raman shifts (455 and 513 cm^{-1}, respectively). The appearance of new peaks could indicate the existence of different TiO_6 octahedra rotation modes on the CCTO perovskite crystals, in agreement with previous dielectric and magnetic observations.[18]

It has been previously shown that the Raman peaks shift to longer wavenumbers in Ti-deficient samples compared to those of (nominally) stoichiometric CCTO.[19] This indicates that an increase in the Cu/Ti ratio leads to a displacement of the Raman peaks to longer wavenumbers. The displacement could be produced by an increase of the crystal's internal pressure as a consequence of the Cu cations incorporation or to changes in the oxidation state of the different atoms on the CCTO composition.

Recently, polar arrangement of electrons on mixed valence states of Cu^{2+}/Cu^{1+} and Ti^{4+}/Ti^{3+} pairs has been proposed to be on the origin of the high dielectric constant behaviour.[20] The existence of Ti^{3+} cations has been confirmed by magnetic measurements and reported to contribute to the anomalous increment of low temperature imanation of this material at temperatures lower than the first relaxation peak of the dielectric constant.[18] The low temperature magnetic response of CCTO has been explained on the basis of the existence of two coupled magnetic contributions, an antiferromagnetic Cu^{2+}–Cu^{2+} superexchange interaction plus a paramagnetic like contribution through the magnetic Ti^{3+}.[18] This mechanism explains also the anomalous antiferromagnetic ordering through the nonmagnetic Ti^{4+} rather than via the usual oxygen coupling proposed by Lacroix.[21]

It has been shown that Cu^{2+} is kinetically reduced to Cu^{1+} at temperatures over 1065 °C. This reduction will mainly take place on the intergranular Cu-rich phase, and could incorporate into the CCTO crystals at long sintering times. These Cu^{1+} ions have previously been observed in CCTO by XPS[22] or as Cu_2O secondary phase by X-ray diffraction.[23] In our case, XANES measurements have been performed at room temperature in open air to study the oxidation state of Cu cations on the sintered samples in volume and its evolution with the sintering time. The results corresponding to the samples sintered for 2 and 32 h are shown in Fig. 5. The main features observed on these XANES spectra can be ascribed to the transitions from 1s level to the different 4pσ and 4pπ levels of Cu^{2+} ions (as signalled on the figure).[24] Moreover, a small peak observed near the absorption edge (at ~2 eV) has been associated to 1s → 3d transition on this same Cu^{2+} ion.[24] The presence of Cu^{1+} ions would be observed by the existence of a single peak at about 10 eV.[25] Though this peak is not observed on our results, its absence could be due to a very small concentration of Cu^{1+} cations, making it difficult to resolve the peak which should appear at half way to the top of the absorption edge. The comparison of both spectra shows the same values at all energies, within the resolution of the experiment, suggesting the absence of significant evolution of the Cu oxidation state with the sintering time. Thus, the changes in the perovskite structure suggested by the Raman spectra cannot be assigned to a reduction effect of the Cu cations.

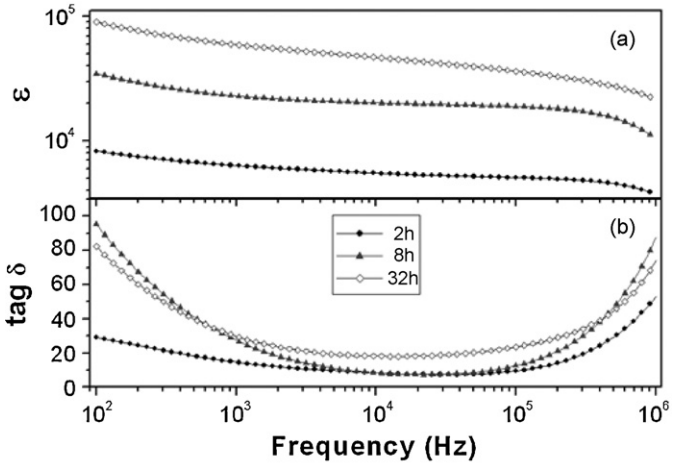

Fig. 6. Frequency dependence of the dielectric constant (a) and, loss tangent (b) for different sintering time samples.

The dependence of the dielectric constant on frequency, measured at room temperature, for samples sintered during different times is shown in Fig. 6. As can be observed, the dielectric constant increases with the sintering time by nearly one order of magnitude, reaching a value of 6×10^4 at 1 kHz in 32 h sintered pellets. The dielectric constant decreases slightly with increasing frequency up to 0.5 MHz. The dielectric losses, shown in Fig. 6b, are high and frequency dependent, showing minimum values in the frequency range 1–100 kHz for all samples. It is interesting to remark that dielectric losses increase with sintering time, especially at low frequencies.

Some authors indicate that the high dielectric constants measured in CCTO samples can be produced by the surface barrier layer capacitor (SBLC) appearing between the samples and the electrodes.[26] The value of the dielectric constant would then depend on the nature of the electrode. In our case, although all measurements were performed using the same contacts, an increase of the dielectric constant with the sintering time is observed (see Fig. 6a). This increase cannot be then related to SBLC, which would be the same in all measured samples, indicating that the variation of the dielectric constant is produced by changes on the CCTO samples produced by the sintering time.

Since it has been shown that Cu cation oxidation state is not changing with the sintering time, the observed increase of the dielectric permittivity should be associated to the reduction of the Cu-rich intergranular phase thickness, as suggested by the IBLC model,[4,8] although the observed Cu cation enrichment of the CCTO crystalline phase could also play a role in this enhancement. The Cu stoichiometry of the materials has been previously reported to be a decisive factor on the dielectric constant of CCTO. In particular, in the case of CCTO ceramics, any deviation from stoichiometry leads to a dramatic decrease of the dielectric constant.[7,27]

Nevertheless, in the case of soft chemistry (coprecipitation) processed samples, the dielectric constant remains high even

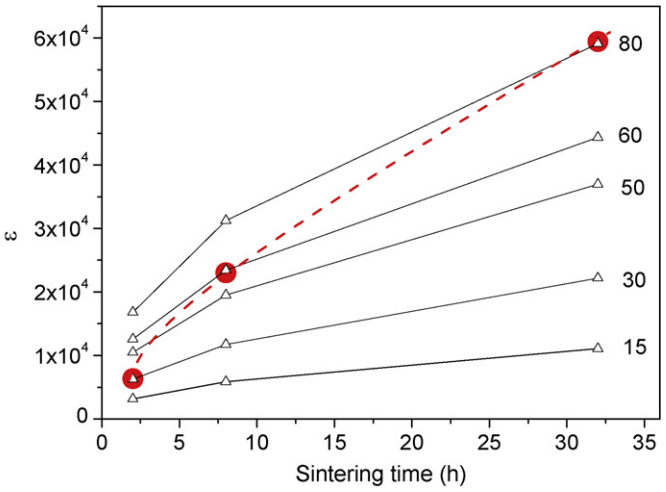

Fig. 7. Evolution of the samples dielectric constant with the sintering time (closed circles, dashed line is a guide for the eyes). The solid lines correspond to the sample, dielectric constant calculated by the IBLC model for different values of the, intergranular dielectric constant (numbers by the lines).

in the presence of Cu cations excess,[28] probably because it is necessary to have a certain amount of secondary phase on the samples to effectively develop the IBLC required microstructure.

In order to evaluate the possible influence of stoichiometry enhancement in the dielectric constant, we have compared the values of the experimentally obtained dielectric constant with those predicted by the IBLC model. We used an IBLC model for a bi-modal distribution of grains, following the expressions obtained on reference.[10]

Though some authors consider that the insulating barrier extends to some extent on the grain borders, we decided to take into account only the previously measured intergranular space (see Fig. 2b), assuming that the insulating layer thickness on the border of the grains would be nearly constant (independent of sintering time). To take into account this layer would only slightly modify the final value of the dielectric constant but not its dependence with sintering time.

The values of the dielectric constant at 1 kHz as a function of sintering time are shown in Fig. 7, together with the values calculated by the bi-modal IBLC model, for different values of intergranular phase dielectric permittivity, ε_b, ranging from 15 to 80. There has not been up to now direct measurements of the dielectric constant of the intergranular phase. Nevertheless, this phase is mainly composed of copper oxide and titanium oxide. The dielectric constant of this material can be obtained by the Maxwell–Wagner equation[29] taking into account the values of the constants corresponding to CuO and TiO_2.[30] The values of the dielectric constant for these materials are 18 and ~90, respectively.

As can be observed in Fig. 7, the experimentally determined dielectric constant does not follow the same trend with sintering time than the IBLC-calculated ε for any single value of the intergranular phase dielectric constant (these values appear next to the calculated curve), even taking into account the uncertainty on the determination of the intergranular thickness. The experimental values increase faster with the sintering time than the calculated values do.

From Fig. 7 it is clear that a change on the dielectric constant of the intergranular phase by an order of 2.7 could explain the variation of the CCTO ceramic samples dielectric constant. The limiting values of the intergranular dielectric constant roughly correspond to those of CuO and TiO_2.[30] Moreover, recent measures of the dielectric constant of TiO_2 doped with small amounts of CuO show values on the order of 90.[31,32] This indicates that the increase of ε_b would correspond to a nearly complete conversion of the intergranular composition from Cu-oxide rich phase (observed to be the main component on samples sintered for 2 h) to Ti oxide rich phase. This conversion of the interphase composition agrees with the observed incorporation of Cu cations from the intergranular phase into the CCTO grains.

4. Conclusions

We have shown that by increasing sintering time at 1100 °C on open air, the dielectric constant of CCTO ceramics increases up to a value of 6×10^4. This increase of the dielectric constant is accompanied by a thickness reduction of the Cu-oxide intergranular phase and a Cu enrichment of the CCTO grains. The Raman spectra show a reduction of the TiO_6 octahedra rotation modes with the sintering time, due to the incorporation of Cu cations into the CCTO crystal lattice. The Cu oxidation state does not change with the sintering time, as demonstrated by XANES measurements. The comparison of the dielectric constant obtained form experimental results and calculated by the IBLC model shows evidence of intergranular phase evolution towards a Ti-rich phase with a higher dielectric constant than the Cu-rich phase that assists the sintering process during early stages.

Acknowledgements

This work was supported by the CSIC project PIF MAGIN and CICYT project MAT2007-66845-C02-01. We acknowledge the European Synchrotron Radiation Facility for provision of synchrotron radiation facilities and we would like to thank F. Jimenez-Villacorta for assistance in using beamline 25 (SPLINE). Dr. J.J. Romero is indebted to CSIC for a "Junta de Ampliación de Estudios" contract (ref. JAEDOC087).

References

1. Subramanian, M. A., Li, D., Duan, N., Reisner, B. A. and Sleight, A. W., High dielectric constant in $ACu_3Ti_4O_{12}$ and $ACu_3Ti_3FeO_{12}$ phases. *J. Solid State Chem.*, 2000, **151**, 323.
2. Fang, L., Shen, M., Yang, J. and Li, Z., The effect of SiO_2 barrier layer on the dielectric properties of $CaCu_3Ti_4O_{12}$ films. *J. Phys. D: Appl. Phys.*, 2005, **38**, 4236–4240.
3. Homes, C. C., Vogt, T., Shapiro, S. M., Wakimoto, S. and Ramirez, A. P., Optical response of high-dielectric-constant perovskite-related oxide. *Science*, 2001, **293**, 636–673.
4. Adams, T. B., Sinclair, D. C. and West, A. R., Giant barrier layer capacitance effects in $CaCu_3Ti_4O_{12}$ ceramics. *Adv. Mater.*, 2002, **14**, 1321–1323.
5. Bochu, B., Deschizeaux, M. N., Joubert, J. C., Collomb, A., Chenavas, J. and Marezio, M., *J. Solid State Chem.*, 1979, **29**, 291.

6. Kant, C., Rudolf, T., Drohnos, S., Lukenheimer, P., Ebbinhaus, S. G. and Loidl, A., Broadband dielectric response of $CaCu_3Ti_4O_{12}$: from dc to the electronic transition regime. *Phys. Rev. B*, 2008, **77**, 045131.
7. Shao, S. F., Zhang, J. L., Zheng, P. and Wang, C. L., Effect of Cu-stoichiometry on the dielectric and electric properties in $CaCu_3Ti_4O_{12}$ ceramics. *Solid State Commun.*, 2007, **142**, 281–286.
8. Wangbo, M.-H. and Subramanian, M. A., Structural model of planar defects in $CaCu_3Ti_4O_{12}$ exhibiting a giant dielectric constant. *Chem. Mater.*, 2006, **18**, 3257–3260.
9. Li, J., Sleight, A. W. and Subramanian, M. A., Evidence for internal resistive barriers in a crystal of the giant dielectric constant material $CaCu_3Ti_4O_{12}$. *Solid State Commun.*, 2005, **135**, 260.
10. Pan, M. J. and Bender, B. A., A bimodal grain size model for predicting the dielectric constant of calcium copper titanate ceramics. *J. Am. Ceram. Soc.*, 2005, **88**, 2611–2614.
11. Fang, L., Shen, M. and Cao, W., Effects of postanneal conditions on the dielectric properties of $CaCu_3Ti_4O_{12}$ thin films prepared on Pt/Ti/SiO_2/Si substrates. *J. Appl. Phys.*, 2004, **95**, 6483–6485.
12. Wu, L., Zhu, Y., Park, S., Shapiro, S. and Shirane, G., Defect structure of the high-dielectric-constant pervoskite $CaCu_3Ti_4O_{12}$. *Phys. Rev. B*, 2005, **71**, 014118.
13. Brizé, V., Gruener, G., Wolfman, J., Fatyeyeva, K., Tabellout, M., Gervais, M. *et al.*, Grain size effects on the dielectric constant of $CaCu_3Ti_4O_{12}$ ceramics. *Mater. Sci. Eng. B*, 2006, **129**, 135–138.
14. Leret, P., Fernandez, J. F., de Frutos, J. and Fernandez-Hevia, D., Nonlinear *I–V* electrical behaviour of doped $CaCu_3Ti_4O_{12}$ ceramics. *J. Eur. Ceram. Soc.*, 2007, **27**, 3901–3905.
15. Chung, S.-Y., Kim, I.-D. and Kang, S.-J. L., Strong nonlinear current–voltage behaviour in perovskite-derivative calcium copper titanate. *Nature Mater.*, 2004, **3**, 774–778.
16. Valim, D., Souza Filho, A. G., Freire, P. T. C., Fagan, S. B., Ayala, A. P., Mendes Filho, J. *et al.*, Raman scattering and X-ray diffraction studies of polycrystalline $CaCu_3Ti_4O_{12}$ under high-pressure. *Phys. Rev. B*, 2004, **70**, 132103.
17. Bozin, E. S., Petkov, V., Barnes, P. W., Woodward, P. M., Vogt, T., Mahanti, S. D. *et al.*, Temperature dependent total scattering structural study of $CaCu_3Ti_4O_{12}$. *J. Phys. Condens. Matter*, 2004, **16**, S5091–S5102.
18. Fernandez, J. F., Leret, P., Romero, J. J., de Frutos, J., de la Rubia, M. A., Martin-Gonzalez, M. S., *et al.*, Existence of two magnetic contributions in pure and doped $CaCu_3Ti_4O_{12}$ giant dielectric constant ceramics. *J. Am. Ceram. Soc.*, doi:10.1111/j.1551-2916.2009.03224.x.
19. Chen, K., Wu, Y., Liao, J., Liao, J. and Zhu, J., Raman and Dielectric spectra of $CaCu_3Ti_{3.9}O_{12}$ ceramics. *Integrated Ferroelectrics*, 2008, **97**, 143–150.
20. Ni, L. and Chen, X. M., Dielectric relaxation and formation mechanism of giant dielectric constant step in $CaCu_3Ti_4O_{12}$ ceramics. *Appl. Phys. Lett.*, 2007, **91**, 122905.
21. Lacroix, C., Crystallographic and magnetic structures of materials with threefold orbital degeneracy: application to $CaCu_3Ti_4O_{12}$. *J. Phys. C*, 1980, **13**, 5125–5136.
22. Kosgi, N., Kondoh, H., Tarima, H. and Kuroda, H., Cu K-edge XANES of $(La_{1-x}Sr_x)_2CuO_4$, $YBa_2Cu_3O_y$ and related Cu oxides: valence, structure and final-state effects on 1s-4pπ and 1s-4pσ absorption. *Chem. Phys.*, 1989, **135**, 149–160.
23. Guillemet-Fritsch, S., Lebey, T., Boulos, M. and Durand, B., Dielectric properties of $CaCu_3Ti_4O_{12}$ based multiphased ceramics. *J. Eur. Ceram. Soc.*, 2006, **26**, 1245–1257.
24. Heald, S. M., Tanquada, J. M., Moodenbaugh, A. R. and Xu, Y., Orientation dependent x-ray absorption near edge studies on high T_c superconductors. *Phys. Rev. B*, 1988, **38**, 761–764.
25. Kau, L. S., Spira-Solomon, D. J., Penner-Habu, J. E., Hodgson, K. O. and Solomon, E. I., X-ray absorption edge determination of the oxidation state and coordination number of copper. Application to the type 3 site in Rhus vernicifera laccase and its reaction with oxygen. *J. Am. Chem. Soc.*, 1987, **109**, 6433–6442.
26. Lunkenheimer, P., Fichtl, R., Ebbinghaus, S. G. and Loidl, A., Nonintrinsic origin of the colossal dielectric constant in $CaCu_3Ti_4O_{12}$. *Phys. Rev. B*, 2004, **70**, 172102.
27. Yeoh, C. K., Ahmad, M. F. and Ahmad, Z. A., Effects of Cu and Ti excess on the dielectric properties of $CaCu_3Ti_4O_{12}$ prepared using a wet chemical method. *J. Alloys Compd.*, 2007, **443**, 155–160.
28. Marchin, L., Guillemet-Fritsch, S., Durand, B., LEvchenko, A. A., Navrotsky, A. and Lebey, T., Grain growth-controlled giant permittivity in soft chemistry $CaCu_3Ti_4O_{12}$ ceramics. *J. Am. Ceram. Soc.*, 2008, **91**, 485–489.
29. Kindgery, W. D., *Introduction to Ceramics* (*2nd ed.*). Wiley, New York, 1976, p. 947.
30. Shannon, R. D., Dielectric polarizabilities of ions in oxides and fluorides. *J. Appl. Phys.*, 1993, **73**, 348–366.
31. Kim, D. W., Park, B., Chung, J.-H. and Hong, K. S., Mixture behaviour and microwave dielectric properties in the low fired TiO_2–CuO system. *Jpn. J. Appl. Phys.*, 2000, **39**, 2696–2700.
32. Shin, C.-K. and Paek, Y.-K., Effect of CuO on the sintering behaviour and dielectric characteristics of titanium dioxide. *Int. J. Appl. Ceram. Technol.*, 2006, **6**, 463–469.